INVERSE UNIFIED POWER QUALITY CONDITIONER

Reza Ghazi
Ferdowsi University of Mashhad –Iran
rghazi@um.ac.ir

Mohamad Hosseini Abardeh
Ferdowsi University of Mashhad –Iran
mohamad.hosseini1@gmail.com

ABSTRACT

The cost of switching devices increases exponentially by increasing their rating. Hence, attractiveness of using unified power quality conditioners (UPQC) is reduced when compensation to be carried out for high power sensitive loads. In this paper, a new configuration for UPQC is presented. Using the fundamental power flow analysis, it is shown that by interchanging the position of series and parallel part of UPQC, the total rating of compensator decreases. To acquire more rating reduction, a new simple control algorithm is presented for voltage compensation by injecting the reactive power. Using numerical simulations, the performance of proposed and conventional configurations is compared to show their operational effectiveness and limitations in different loads and network conditions.

INTRODUCTION

Active power filters (APFs) have been used in three last decades to compensate the voltage and current quality problems. Parallel active power filters (PAPFs) can eliminate current distortions caused by loads and perform power factor correction. On the other hand, to protect sensitive consumers from voltage distortions, series active power filters (SAPFs) are used [1].

There exist four trends to enable the more efficient utilization of APFs for protecting the high power loads and networks against power quality disturbances. They are as follows. 1) Improvement of manufacturing technology of APF's semiconductor switches to reduce their cost and to increase their rating. 2) Application of hybrid configurations of active and passive power filters [2]. 3) Using the selective harmonic compensation control algorithms to minimize the rating of series and parallel APFs [3]. 4) Optimization of APF power flow by using the energy optimized control algorithms [4], [5]. In order to obtain an optimized rating of UPQC, a modified configurations along with a new control approach is proposed in this paper. The conventional UPQC (Fig. 1 (a).) in which the series part is at the network side is compared with an Inverse Unified Power Quality Conditioner (I-UPQC) where the series part is at the load side as shown in Fig. 1 (b).

RATING ANALYSIS

Rating of UPQC and I-UPQC can be calculated by fundamental frequency power flow analysis.

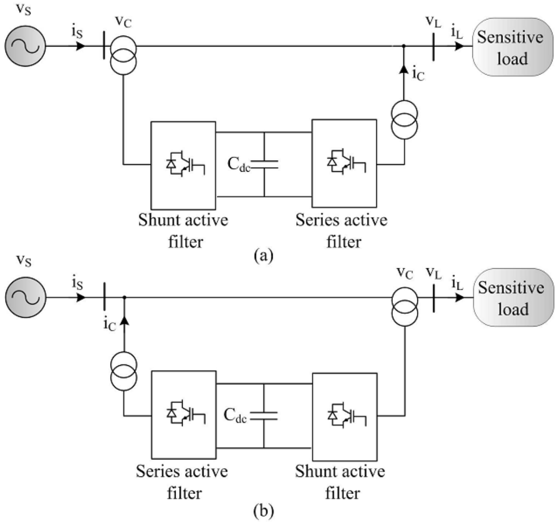

Fig. 1. Configuration of (a) UPQC and (b) I-UPQC

Here due to space limitation, only the results are presented. As shown in Fig. 2 rating of the UPQC increases with increasing the level of voltage sag and the load power factor. The rating of I-UPQC in active power injection mode is higher than that of UPQC whereas in reactive power injection mode, has lower rating especially for power factors near unity.

Generally, I-UPQC in active power injection mode needs lower rating for compensation of same voltage sag among four cases. With regard to rating, the following results are provided upon which the proper choice for sag compensation under different values of power factors can be made.

1. If load has a poor power factor (near 0.5), using I-UPQC with reactive power injection mode will lead to lowest rating.
2. If load has a high power factor (near unity), using I-UPQC or UPQC with active power injection mode will lead to lowest rating. However, for deep voltage sags I-UPQC has lower rating in compare with UPQC.
3. If load has a moderate power factor (between high and low, around 0.7) and the voltage sag factor is below 0.4, UPQC with reactive power injection yields lowest rating.

REFERENCE WAVEFORM ESTIMATION STRATEGY

Reference waveforms of shunt and series active power filters of I-UPQC and UPQC types can be estimated utili-

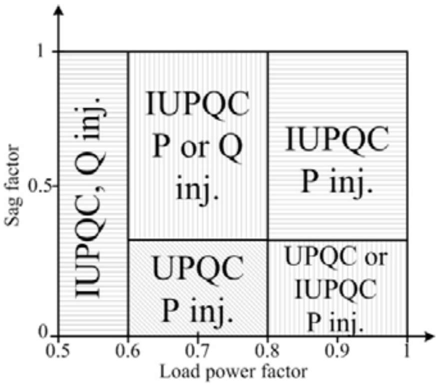

Fig. 2. The lowest rating for different sag factor and load power factor cases (P: active power injection, Q: reactive power injection).

zing various methods. Here a method based on instantaneous reactive power theory is used to generate reference waveforms of the PAPF. An algorithm based on the synchronous reference frame transformation is presented to estimate the reference waveforms of the SAPF. This method can generate the proper waveforms for both active and reactive power injection cases.

SAPF Waveform Estimation

Reference waveforms of series part of power quality compensator are the difference between actual voltage of the network and the load ideal voltage according to IEEE-519 standard. An algorithm based on the synchronous reference frame transformation is used to generate reference waveforms of SAPF. This method is a modified version of algorithm presented in [6].

In Phase Voltage Injection

Considering the instantaneous phaser of network voltage (ωt) as a reference angle, to regulate the load voltage by injecting an in phase voltage, the ideal source voltage in the synchronous reference frame becomes

$$v^{*}_{Sdqo} = [V_m \quad 0 \quad 0]^T \tag{1}$$

and the reference voltage of SAPF equals

$$v^{*}_{cdqo} = v^{*}_{Sdqo} - v_{Sdqo} \tag{2}$$

To obtain the three phase reference voltages, v^{*}_{cdq0} are transformed into three phase space. Fig. 3 shows the block diagram of the proposed algorithm.

Orthogonal Voltage Injection

Considering orthogonality of d and q axes in the synchronous reference frame, to obtain the voltage compensation by injecting reactive power, the injected voltage should be in phase with q-axis. In the case of using UPQC, due to the PAPF operation, the source current and voltage are in phase. Hence, if the injected voltage is orthogonal to the source voltage, it is also orthogonal to the source current, so the reactive power injection is provided. Supposing V_m to be the ideal magnitude of the load voltage, the reference voltage of the orthogonal method can be calculated as below.

$$v^{*}_{cd} = v^{*}_{sd} \tag{3}$$

$$v^{*}_{cq} = \sqrt{V^{2}_{m} - v^{*}_{sd}} \tag{4}$$

Fig. 4 shows the block diagram of the SAPF reference waveform estimation when the injected voltage is orthogonal to the source current.

Fig. 5 shows this active power as a function of voltage sag magnitude (x) and the load power factor. By using the orthogonal voltage algorithm, the injection of active power is less in compare with the in phase method when the sag factor x is above 0.3 p.u. and the power factor is below 0.9. However the maximum of injected active power is less when in phase method is used. To reduce the active power which is injected by SAPF, the angle between fundamental component of the load current and the source voltage (power factor) must be known.

PAPF Waveform Estimation

Assuming the vectors of the network voltage and the load current as

$$\bar{v}_s = [v_{sa} \quad v_{sc} \quad v_{sc}]^T \tag{5}$$

$$\bar{i}_l = [i_{la} \quad i_{lc} \quad i_{lc}]^T \tag{6}$$

$$p = v_{sa} i_{la} + v_{sb} i_{lb} + v_{sc} i_{lc} \tag{7}$$

the active and reactive power of load are equal to the dot and cross product of voltages and currents respectively, i.e.,

$$p = v_{sa} i_{la} + v_{sb} i_{lb} + v_{sc} i_{lc} \tag{8}$$

$$q = \vec{v}_s \times \vec{i}_l = [q_a \quad q_b \quad q_c]^T \tag{9}$$

the mean reactive power is defined as

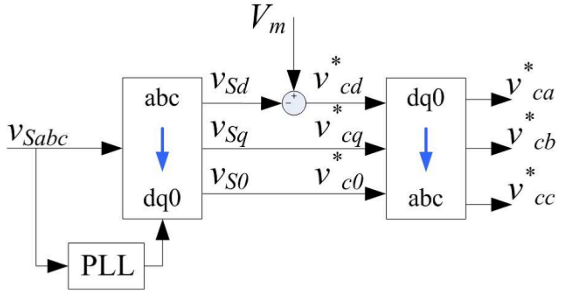

Fig. 3. Block diagram of SAPF reference waveform generation (in phase voltage injection).

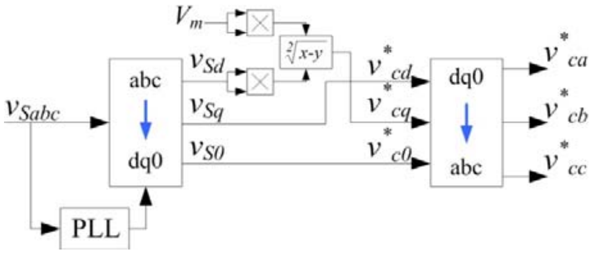

Fig. 4. Block diagram of SAPF reference waveform generation (orthogonal voltage injection).

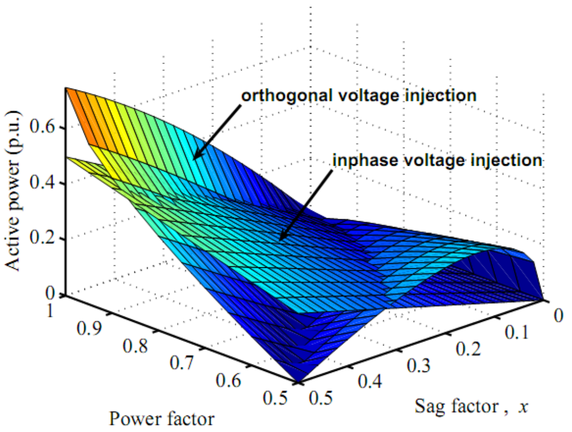

Fig. 5. Comparison between active power injected into the network using in phase and orthogonal voltage injection method.

$$q_{ave} = \frac{v_{sa}(i_{lb} - i_{lc}) + v_{sb}(i_{lc} - i_{la})}{\sqrt{3}} + \frac{v_{sc}(i_{la} - i_{lb})}{\sqrt{3}} \tag{10}$$

Active and reactive power consist of a constant and an oscillatory component as

$$p = \bar{p} + \tilde{p} \tag{11}$$

$$q = \bar{q} + \tilde{q} \tag{12}$$

where $\bar{p}$ and $\bar{q}$ are constant and $\tilde{p}$ and $\tilde{q}$ are the oscillatory components.

In Phase Voltage Injection

Assuming that the PAPF compensates all reactive power demand of the load, by generating q, and also compensates the oscillatory active power of the load current by generating $\tilde{p}$. Hence, $\tilde{p}$ is estimated by passing p through a low pass filter. The voltage at DC link capacitor to be kept constant for achieving the proper compensation [8]. Hence, PAPF should draw additional active power from network to regulate the DC link capacitor voltage. Swings in capacitor voltage are due to distortions exist in network voltage, internal switching and the copper losses of transformer. The voltage error which is difference between the actual capacitor voltage and its reference is fed into a PI controller. This controller estimates the required amount of active power (p_{loss}) for regulating the capacitor voltage. The total active power drawn by PAPF is defined by (12)

$$p_T = \tilde{p} + p_{loss} \tag{13}$$

Reference currents of three phases of the shunt active power filter are obtained by (14) and the block diagram is shown in Fig. 6.

$$i^*_{ca} = i_{la} - \frac{p_T}{v_a^2 + v_b^2 + v_c^2} v_{sa}$$

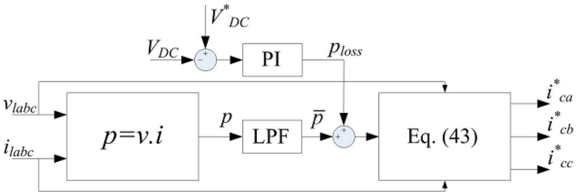

Fig. 6. Shunt active power reference waveform estimation for in phase voltage injection.

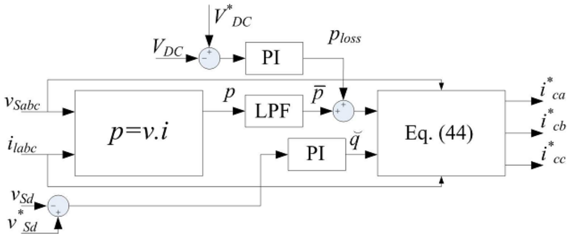

Fig. 7. Shunt active power reference waveform estimation for orthogonal voltage injection.

$$i^*_{ca} = i_{lb} - \frac{p_T}{v_a^2 + v_b^2 + v_c^2} v_{sb} \tag{14}$$

$$i^*_{ca} = i_{lc} - \frac{p_T}{v_a^2 + v_b^2 + v_c^2} v_{sc}$$

If the PAPF of the power quality conditioner injects these currents into the network, the harmonics and the reactive component of the load will diminish, and the DC link voltage is kept constant.

Orthogonal Voltage Injection

The algorithm described in the previous section compensates the reactive power considering that the load and the source voltages are in phase. By using the orthogonal voltage injection, the load voltage leads the source during voltage sag. This will lead to injection or absorption of extra reactive power into/from the network by PAPF. Over rating of PAPF and unwanted distribution network reaction such as over voltage is the result. To solve this problem, a PI controller is used for estimation of additional reactive power. The error voltage i.e. the difference between amplitude of the source voltage in d-axis and its nominal value is fed into this controller and the output is considered as an extra reactive power.

Assuming $\breve{q}$ as the output of PI controller, reference waeforms of PAPF are as follows

$$i^*_{ca} = i_{la} - \frac{p_T}{v_a^2 + v_b^2 + v_c^2}(v_{sa} \cdot p_T + \frac{\breve{q}}{3}(v_{sc} - v_{sb}))$$

$$i^*_{ca} = i_{lb} - \frac{p_T}{v_a^2 + v_b^2 + v_c^2}(v_{sb} \cdot p_T + \frac{\breve{q}}{3}(v_{sa} - v_{sc})) \tag{15}$$

$$i^*_{ca} = i_{lc} - \frac{p_T}{v_a^2 + v_b^2 + v_c^2}(v_{sc} \cdot p_T + \frac{\breve{q}}{3}(v_{sb} - v_{sa}))$$

Fig. 7 shows the block diagram of the reference waveform generation algorithm for PAPF.

SIMULATION RESULTS

Using PSCAD/EMTDC software package, two configurations of power quality conditioners under the control of the aforementioned algorithms are simulated. A full-bridge three phase rectifier is used as a nonlinear load and simulations are performed at 20 kV level.

Fig. 8 shows the load current and the source current after compensation made by UPQC and I-UPQC. The load current comprises a large amount of harmonics with order 6n±1; n = 1, 2, 3,… . The magnitude of the load current harmonics is 20% for 5th and 8% for 7th harmonic. The compensated source current is nearly sinusoidal having THD about 1.3% and 1.7%, respectively in UPQC and I-UPQC.

To assess the compensator performance in voltage compensation by injecting orthogonal voltage, a voltage sag as deep as 25%, started at t = 0.1 sec is supposed. Fig. 9 shows the load voltages after compensation made by UPQC and I-UPQC. The load voltage is regulated, however a phase jump about 41° is observed at the beginning of the voltage sag.

CONCLUSION

Using the mathematical representations it is shown that if the series part of UPQC is interchanged with its shunt part such that the series part is located at load side (known as I-UPQC), the total rating of the compensator will be reduced when the load draws a large amount of reactive power from the network. Further rating reduction is possible by using the reactive power injection for voltage regulation.

A new algorithm has been presented for generating reference waveforms of the UPQC and the I-UPQC for orthogonal voltage injection to avoid the phase jump.

Numerical simulations show that the I-UPQC can perform power quality compensation using conventional control algorithm if the network voltage does not contain a significant unbalance or harmonic.

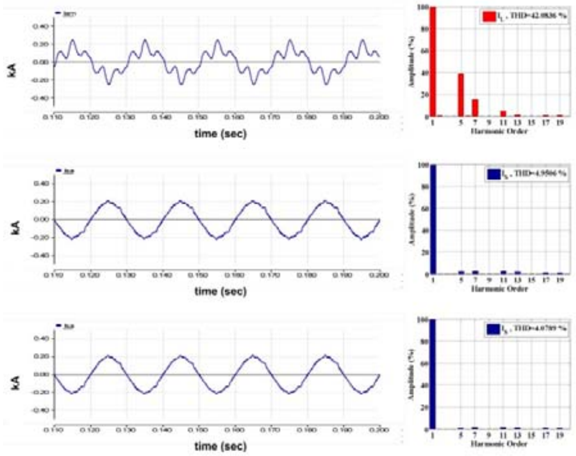

Fig. 8. From top to bottom: load current, source current compensated by UPQC, source current compensated by I-UPQC.

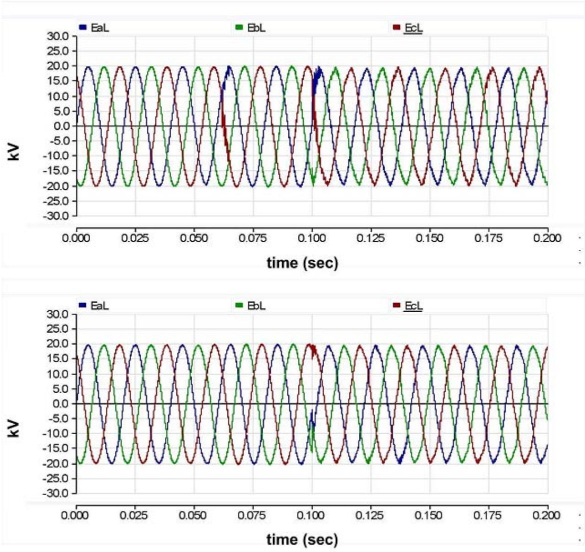

Fig. 9. Voltage compensation using orthogonal voltage injection; load voltage compensated by UPQC (top), load voltage compensated by I-UPQC (bottom).

REFERENCES

[1] G. J. Nilesen and F. Blaabjerg, “A detailed comparison of system topologies for dynamic voltage restorer,” *IEEE Transaction on Industry Application*, vol. 41, no. 5, pp. 1272–1280, September/October 2005.

[2] B. Singh, K. Al-Haddad, and A. Chandra, “A review of active filters for power quality improvement,” *IEEE Transaction on Industrial Electronics*, vol. 46, no. 5, p. 960- 971. 1999.

[3] P. Mattavelli, “A closed-loop selective harmonic compensation for active filters,” *IEEE Transaction on Industy Application*, vol. 37, no. 1, pp. 81–89, January/February 2001.

[4] Y. Y. Kolhatkar and S. P. Das, “Experimental investigation of a single phase UPQC with minimum VA loading,” *Electric Power System Research*, vol. 77, pp. 821–830, March/April 2007.

[5] H. Fujita and H. Akagi, “The unified power quality conditioner: the integration of series and shunt active power filters,” *IEEE Transaction on Power Electronics*, vol. 13, no. 2, pp. 315–322, March 1998.

[6] M. Basu, S. P. Das, and G. K. Dubey, “Comparative evaluation of two models of UPQC for suitable interface to enhance power quality,” *Electric Power System Research*, vol. 77, pp. 821–830, March/April 2007.

[7] J. Tutunen, M. Salo, and H. Tuusa, “The influence of the DC-link voltage control on the current harmonic filtering of the series hybrid active filters,” in *31th Annual Conference on Industrial Electronics Society*, 2005, pp. 918–923.